All-sky gravitational wave burst search in the Virgo C7 run data

F. Acernese[6], P. Amico[10], M. Alshourbagy[11], F. Antonucci [12], S. Aoudia[7], P. Astone[12], S. Avino[6], D. Babusci[4], G. Ballardin[2], F. Barone[6], L. Barsotti[11], M. Barsuglia[8] , Th. S. Bauer[13], F. Beauville[1], S. Bigotta[11], S. Birindelli[11], M.A. Bizouard[8], C. Boccara[9], F. Bondu[7], L. Bosi[10], C. Bradaschia[11], S. Braccini[11], F. J. van den Brand[13],A. Brillet[7], V. Brisson[8], D. Buskulic[1], E. Calloni[6], E. Campagna[3], F. Carbognani[2], F. Cavalier[8], R. Cavalieri[2], G. Cella[11], E. Cesarini[3], E. Chassande-Mottin[7], N. Christensen[2], C. Corda[11], A. Corsi[12], F. Cottone[10], A.-C. Clapson[8], F. Cleva[7], J.-P. Coulon[7], E. Cuoco[2], A. Dari[10], V. Dattilo[2], M. Davier[8], M. del Prete[11], R. De Rosa[6], L. Di Fiore[6], A. Di Virgilio[11], B. Dujardin[7], A. Eleuteri[6], M. Evans[2], I. Ferrante[11], F. Fidecaro[11], I. Fiori[2], R. Flaminio[1,2], J.-D. Fournier[7], S. Frasca[12], F. Frasconi[11], L. Gammaitoni[10], F. Garufi[6], E. Genin[2], A. Gennai[11], A. Giazotto[11], G. Giordano[4], L. Giordano[6], R. Gouaty[1], D. Grosjean[1], G. Guidi[3], S. Hamdani[2], S. Hebri[2], H. Heitmann[7], P. Hello[8], D. Huet[2], S. Karkar[1], S. Kreckelbergh[8], P. La Penna[2], M. Laval[7], N. Leroy[8], N. Letendre[1], B. Lopez[2], Lorenzini[3], V. Loriette[9], G. Losurdo[3], J.-M. Mackowski[5], E. Majorana[12], C. N. Man[7], M. Mantovani[11], F. Marchesoni[10], F. Marion[1], J. Marque[2], F. Martelli[3], A. Masserot[1], M. Mazzoni[3], L. Milano[6], F. Menzinger[2], C. Moins[2], J. Moreau[9], N. Morgado[5], B. Mours[1], F. Nocera[2], C. Palomba[12], F. Paoletti[2], 11, S. Pardi[6], A. Pasqualetti[2], R. Passaquieti[11], D. Passuello[11], F. Piergiovanni[3], L. Pinard[5], R. Poggiani[11], M. Punturo[10], P. Puppo[12], S. van der Putten[13], K. Qipiani[6], P. Rapagnani[12], V. Reita[9], A. Remillieux[5], F. Ricci[12], I. Ricciardi[6], P. Ruggi [2], G. Russo[6], S. Solimeno[6], A. Spallicci[7], M. Tarallo[11], M. Tonelli[11], A. Toncelli[11], E. Tournefier[1], F. Travasso[10], C. Tremola[11], G. Vajente [11], D. Verkindt[1], F. Vetrano[3], A. Viceré[3], J.-Y. Vinet[7], H. Vocca[10] and M. Yvert[1]

[1]*Laboratoire d'Annecy-le-Vieux de Physique des Particules (LAPP), IN2P3/CNRS, Université de Savoie, Annecy-le-Vieux, France;*

[2]*European Gravitational Observatory (EGO), Cascina (Pi), Italia;*

[3]*INFN, Sezione di Firenze/Urbino, Sesto Fiorentino, and/or Università di Firenze, and/or Università di Urbino, Italia;*

[4]*INFN, Laboratori Nazionali di Frascati, Frascati (Rm), Italia;*

[5]*LMA, Villeurbanne, Lyon, France;*

[6]*INFN, sezione di Napoli and/or Università di Napoli "Federico II" Complesso Universitario di Monte S.Angelo, and/or Università di Salerno, Fisciano (Sa), Italia;*

[7]*Departement Artemis – Observatoire de la Côte d'Azur, BP 42209 06304 Nice, Cedex 4, France;*

[8]*LAL, Univ Paris-Sud, IN2P3/CNRS, Orsay, France*

[9]*ESPCI, Paris, France;*

[10]*INFN, Sezione di Perugia and/or Università di Perugia, Perugia, Italia;*

[11]*INFN, Sezione di Pisa and/or Università di Pisa, Pisa, Italia;*

[12]*INFN, Sezione di Roma and/or Università "La Sapienza", Roma, Italia;*

[13]*NIKHEF, NL-1009 DB Amsterdam and/or Vrije Universiteit, NL-1081 HV Amsterdam, The Netherlands.*

We report on a search for Gravitational Wave (GW) bursts in the Virgo C7 commissioning run. The search focused on unmodeled short duration signals in the frequency range 150Hz to 2 kHz. An extensive understanding of the data set has been carried out to be able to handle a burst search using the output of only one detector. No GW burst candidates differing from the background were identified. A 90% confidence level upper limit on the number of expected events given the Virgo C7 sensitivity curve has been derived as function of the signal strength. The sensitivity of the analysis presented is, in terms of the root sum square strain amplitude, $\sim 10^{-20}/\sqrt{Hz}$.

1 Introduction

Gravitational Wave (GW) bursts are all possible signals whose duration is short, less than a few hundred of milliseconds. The astrophysical sources are various: massive star core collapse, the merging phase of coalescing compact binary systems forming a single black hole, black hole ring-

down, astrophysical engines that generate gamma-ray burst, neutron star oscillation modes and instabilities, and cosmic string cusps and kinks. See references in [1]. Some are well modeled, but not all such that a burst pipeline is built making very few assumption on the source waveforms.

Virgo[2] is a 3-km long arm power-recycled Michelson interferometer located in Pisa, Italy. Its commissioning started in 2003 and regular data taking campaigns have been organized after each important milestone. The last commissioning run (C7) took place in September 2005 lasting for 5 days, when Virgo was running in its final optical recycled configuration. The best achieved sensitivity was $h = 7 \times 10^{-22}/\sqrt{Hz}$ at 300 Hz.

The C7 run data has been used for extensive analysis of the Virgo noise [3] [4] which is a fundamental step to perform a GW burst search with only one detector. One of the difficulties of a GW burst search carried out in only one detector is the high false alarm rate due to the numerous sources of glitches and non stationary data. In a multi-interferometer search they can be discarded by requesting that the event be seen in coincidence in the detectors.

2 Pipeline overview

The Exponential Gaussian Correlator (EGC) produces a time-frequency representation of the data by applying the correlation relation for a list of templates of the same family:

$$\Phi_{f_0,Q_0}(t) = e^{-2(\pi f_0/Q_0)^2 t^2} e^{i2\pi f_0 t} \tag{1}$$

with (f_0, Q_0) the central frequency and quality factor of the template. The correlation between the data $x(t)$ and a template is simply given by:

$$C_{f_0,Q_0}(t) = \frac{1}{\sqrt{2\pi}} \frac{Q}{f_0} \int_{-\infty}^{+\infty} \frac{e^{-(\frac{f-f_0}{f_0})Q^2/2} \times \tilde{x}(f)}{S_h(f)} e^{i2\pi f t} df \tag{2}$$

where $\tilde{x}(f)$ is the Fourier transform of $x(t)$ and $S_h(f)$ is the one-sided power spectral density. $C(t)$ is a complex function whose square modulus defines an energy E. The Signal to Noise Ratio is just given by SNR $= \sqrt{2 \times E}$.
Template selection relies on a tiling algorithm valid for any two-parameter matched filter bank. The tiling zone has been chosen in order to cover with a minimal match of 99% oscillatory waveforms whose parameters are 150Hz $\leq$ f $\leq$ 2kHz and $2 \leq$ Q ≤ 16, which correspond to the C7 Virgo frequency band of best sensitivity. Events whose energy exceeds a threshold of 5.4 are then clusterized in the time-frequency plane and the SNR, the GPS time and the frequency of the event are given by the template having the maximal SNR in the cluster. More details can be found in [5]. In this analysis, trigger lists are produced by selecting all events whose SNR is above 5.

3 Data selection

The first step of the analysis consists in defining the so-called science segments of data: the interferometer is locked, thermal resonances are damped, and the last 10 seconds before the loss of lock are suppressed such that the burst pipeline output is not biased by the large oscillation of the control signals which usually generate the loss of lock. This selection reduces the C7 duty cycle (when the interferometer is locked) from 65.8% to 57.9%. Then, inside each segment some bad data quality periods (corresponding to obvious instrumental malfunctioning such as photodiode saturation [3]) have been identified. Some data quality (DQ) veto segments have been produced. These DQ vetoes are applied on the list of event triggers. The dead time induced is 0.8%. Then, starting from the remaining triggers, we tried to understand the origin of the events having high SNR value. Two categories of loud triggers have been identified; the first

one, corresponds to events that are due to an external source of noise. For instance, acoustic noise is generated by the picomotors used to realign the quadrant photodiodes on the external detection bench. Other transient signals were due to glitches in some control signals, especially the correction signal of the loop to stabilize the laser frequency. All these strain amplitude glitches have been found to be in coincidence with glitches or RMS increases in other auxiliary channels: some acoustic probe channels ("DB"), the laser frequency correction channel ("SSFS") and the DC power from the light heading back to the laser source ("B2"). Three event by event vetoes have been developed and optimized [3]. The dead time due to these vetoes is of order 6%. The second category of loud triggers have been found to be due to non stationary data periods, lasting up to a few seconds. It turns out that the mirrors' alignment control system was not optimally working during C7 and the angular tilts of the mirrors induce an increase of the coupling of the laser frequency noise with the GW strain amplitude signal. The period of this non stationary feature is 27 s, corresponding to the period of a mechanical resonance in the Virgo mirror suspension system. The main characteristics of the burst events generated by these non-stationarities are their rather long duration (up to a few seconds after clusterization) and their broad frequency content, which proves their laser frequency noise origin. These events have a continuous SNR distribution, with the majority of them having a moderate SNR. They are actually dominating the excess of burst events, justifying the need to develop an efficient veto to suppress them. By monitoring a specific line that is introduced in the laser source system at 1111 Hz in order to measure the laser frequency noise level in the dark fringe, one could see the coincidence between the GW strain amplitude non stationary features and an amplitude increase of the 1111 Hz line. The dead time induced by this veto ("1111Hz") amounts to 16%. This is admitely large but actually is compatible with the oscillation period of the mirrors which is the origin of the non stationary noise.

Finally, after applying all the vetoes we ended up with a very loud trigger (SNR=70) showing a perfect sine Gaussian form. This event has been thoroughly studied and it was discovered that it is observable in the other frequency demodulation phase dark fringe channel with an even stronger SNR value (SNR=140). This is totally incompatible with what is expected for a real GW event. A veto ("PQ") checking the relationship between the two demodulation phase strengths has been developed.

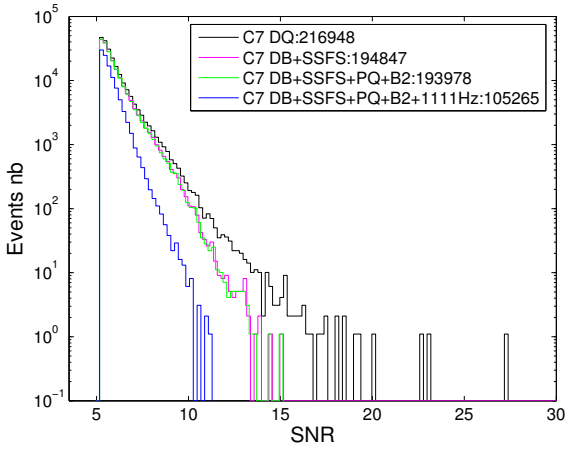

Figure 1: SNR distributions of the EGC GW burst triggers obtained in the full C7 data set at different steps of the application of the vetoes. "DB", "SSFS", "PQ" and "B2" refer to vetoes which suppress transient events due to a glitch in an auxiliary channel, while the "1111Hz" veto is used to suppress the non stationary data periods due to the mirror's large tilt amplitude.

The resulting dead time of all the vetoes applied amounts to 20.1% taking into account that some veto segments may overlap. The effect of the application of all the vetoes on the EGC C7

triggers is shown in Figure 1. One can see that the anti-glitch vetoes ("DB", "SSFS", "B2" and "PQ") mainly suppress the loudest background events, while the "1111Hz" veto mainly acts on the core of the SNR distribution. 97% of the EGC triggers with SNR above 10 are suppressed by the vetoes. Only 12 triggers above SNR=10 remain. The loudest SNR is 11.2.

4 Results and conclusion

In the end, the GW burst search in C7 data results with no GW candidate. An upper limit on the detectable number of events can be calculated. Assuming no background events and considering an effective data set duration of 1.96 days, the frequentist upper limit at 90% confidence level is $-ln(1-.9)/1.96 = 1.17$ events per day. This rate depends on the type of GW sources which are searched for and the efficiency of the pipeline to detect them.In this analysis, we have considered that the sources are randomly distributed over the sky. The efficiency of the analysis pipeline has been estimated by injected artificially linearly polarized Sine Gaussian waveforms whose central frequency is in the 150-2000 Hz analysis band. The polarization angle is random and the signals are added to the C7 data at random GPS times with different amplitude values given by the root-sum-squared strain amplitude: $h_{rss} = \sqrt{\int |h(t)|^2 dt}$. The efficiency of the EGC pipeline for a given h_{rss} is given by the fraction of events detected with a SNR larger to 11.2. This threshold corresponds to a zero-background search. The efficiency as a function of the h_{rss} is fitted using a sigmoid function. The frequentist upper limit at 90% confidence level on the detectable number of events as function of the strain amplitude is then derived. Figure 2 shows the upper limit for four Sine Gaussian signals spanning the frequency analysis band.

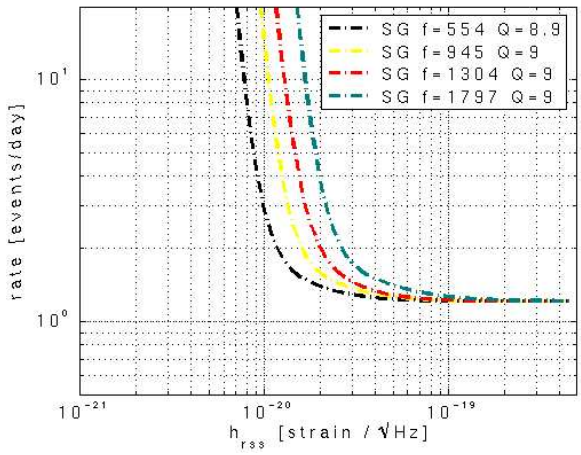

Figure 2: Upper limit at 90% confidence level on the number of detectable events as function of the strain amplitude for four SineGaussian signals, obtained in the C7 data.

The sensitivity to generic GW burst signals (Sine Gaussian waveforms) has been estimated to be $1 - 2\ 10^{-20}/\sqrt{Hz}$. This can be translated into a limit on the GW energy emitted for instance by a source at the center of the Galaxy of $1.6\ 10^{-6} M_{\odot}$.

References

1. F. Beauville *et al*, submitted to *Phys. Rev.* D, arXiv gr-qc/0701026
2. G. Vajente (for the Virgo Collaboration), XI^{th} GWDAW, Postdam (2006)
3. F. Cavalier (for the Virgo Collaboration), these proceedings
4. I. Fiori, N. Christensen (for the Virgo Collaboration), XI^{th} GWDAW, Postdam (2006)
5. A.-C. Clapson *et al*, submitted to *Phys. Rev.* D